

Journal of Thermoplastic Composite Materials

<http://jtc.sagepub.com/>

Multiwalled Carbon Nanotube/Polysulfone Composites

Thomas Dooher, Dorian Dixon and Alistair McIlhagger

Journal of Thermoplastic Composite Materials published online 31 December 2010

DOI: 10.1177/0892705710391621

The online version of this article can be found at:

<http://jtc.sagepub.com/content/early/2010/11/24/0892705710391621>

Published by:



<http://www.sagepublications.com>

Additional services and information for *Journal of Thermoplastic Composite Materials* can be found at:

Email Alerts: <http://jtc.sagepub.com/cgi/alerts>

Subscriptions: <http://jtc.sagepub.com/subscriptions>

Reprints: <http://www.sagepub.com/journalsReprints.nav>

Permissions: <http://www.sagepub.com/journalsPermissions.nav>

Multiwalled Carbon Nanotube/Polysulfone Composites

Thomas Dooher, Dorian Dixon* and Alistair McIlhagger

*University of Ulster, Jordanstown Campus, Shore Road, Newtownabbey,
Co. Antrim, BT37 0QB, UK*

ABSTRACT: The solution method was used to create polysulfone/carbon nanotubes composites. The effect of three solvents (NMP, DMF, and THF), treatments (nitric acid and ethanol) and surfactants (ODA and OCA) on CNT/solvent stability was investigated. NMP and DMF resulted in improved stability compared to THF, and all CNT treatments improved stability. Four composites were produced with CNT loadings of 0–5 wt%: as-received CNT and nitric acid treated in THF, as-received CNT and OCA surfactant CNT in NMP. Optical, TEM, and electrical percolation measurements confirmed the role of CNT/solvent stability on the final composite dispersion. Tensile testing and thermal analysis confirmed the presence of residual solvent in all samples.

KEY WORDS: polysulfone, carbon nanotubes, solution method.

INTRODUCTION

SINCE THEIR DISCOVERY by Iijima in 1991 [1], carbon nanotubes have been the subject of a concerted international research effort. With a recorded Young's modulus and tensile strength for multi-walled carbon nanotubes of 1.28 TPa [2] and 63 GPa [3], respectively, they are amongst the strongest and stiffest materials yet discovered. In addition to exceptional mechanical performance, CNTs possess other unique properties such as high current densities (2.4×10^8 A/cm²) [4], a thermal stability of around 700°C in air [5] and exceptional chemical resistance [6]. However, due to their size with diameters in the nanometer range and length ranging from a few

*Author to whom correspondence should be addressed. E-mail: d.dixon@ulster.ac.uk
Figures 6 and 7 appear in color online <http://jtc.sagepub.com>

microns to millimeters [7], it is not possible to fabricate bulk products directly from CNT. A commonly employed technique to exploit these exceptional properties in bulk materials is via CNT/Polymer composites.

While several high profile applications exploiting the mechanical performance of CNT exist such as the 2005 bike which won the Tour de France [8], commercial production of CNT reinforced polymers has so far been limited to several companies marketing CNT masterbatches that impart electrical conductivity at low addition rates [9]. In addition to their high cost and health and safety concerns the two main factors limiting the performance and hence application of CNT/polymer composites are inadequate dispersion and interfacial bonding issues [10].

Strong van der Waals interactions between individual tubes coupled with their large aspect ratios leads to CNT clumping [11]. These agglomerates can act as crack initiation sites and reduce mechanical performance. Interfacial bonding is also critical, as poor CNT/matrix bonding limits the transfer of externally applied loads to the CNT. A wide range of methodologies have been employed to overcome these two issues. These include suspending the CNT in a suitable solvent [12], surfactants [13], surface functionalization through the attachment of various moieties such as COOH via acid treatment [14] or through the use of high shear melt processing.

A solvent casting approach [15] has been adopted for this study on CNT/polysulfone composites. Solvent casting tends to result in enhanced dispersion and mechanical performance compared to melt processed samples, and is suitable for low volume laboratory studies [16]. The method provides a convenient method to screen a large number of CNT functionalization approaches. In addition, high loading levels are possible since the addition of nanotubes (or other nanoscale reinforcement) increases the viscosity of a material which limits the loading levels achievable in melt processing [8].

Due to issues relating to dispersion and interfacial bonding, realizing the potential gains in mechanical performance possible with CNT/polymer composites is difficult with many studies reporting reduced strength and stiffness with the addition of CNT [17–19]. However, several studies have reported improvements. In 2002, Cadek et al. reported an increase in Young's modulus of a factor of 1.8 in PVA [20] and in 2004 reported an increase in Young's modulus of a factor of 2 using PVA again [21]. From the same group, Coleman et al. reported a 3.7-fold increase in the Young's modulus of PVA and a 3.1-fold increase in Young's modulus of polypropylene using CNT, which had chlorinated polypropylene covalently bonded to their surface [22]. Dufresne et al. reported a linear increase in the Young's modulus with increasing wt% of CNTs (achieving an almost 7-fold increase with 15 wt%) [23] and Qian et al. reported an increase in Young's

modulus of 42% [24]. Safadi et al reported an increase of a factor of 2.2 using polystyrene [25]. The presence of CNT can also alter the mechanical performance by increasing crystallinity through nucleating effects.

Polysulfone is a yellow, transparent, high temperature, engineering thermoplastic with a high glass transition temperature ($\sim 185^{\circ}\text{C}$). Applications include autoclavable medical devices, underhood automotive components, and printed circuit board devices [26]. To the authors' knowledge, CNT/polysulfone composites for mechanical and electrical applications have not been previously reported, with the only previous studies investigating polysulfone/CNT composites for gas membranes [27] and immunosensors [28]. Whilst an extensive body of published studies has investigated CNT/thermoplastic composites, the majority of this work has concentrated on high volume commodity thermoplastics such as polyethylene, polypropylene and nylon, or water soluble polymers such as poly vinyl alcohol. The addition of CNT to high temperature thermoplastics such as those in the sulfone group (polysulfone, polyethersulfone, polyphenylsulfone) offer the promise of enhanced thermal stability and fire retardancy, in addition to electrical conductivity and improved mechanical performance.

MATERIALS AND METHODS

Multi-walled CNT (MWCNT) were purchased from Shenzhen Nanotech Port Co. Ltd, (diameter 10–20 nm, length 5–15 μm and purity of 95–98%). The polysulfone was obtained from Solvay Advanced materials and is marketed under the trade name UDEL grade P-1800-NT. All other chemicals were obtained from Sigma-Aldrich and used as received. Tetrahydrofuran (THF) (purity $\geq 99.0\%$), N, N-Dimethylformamide (DMF) (purity 99%) and 1-methyl-2-pyrrolidone (NMP) (purity $\geq 98\%$) were used without further purification. Two amine terminated alkanes surfactants: octylamine (OCA) (purity $\geq 99\%$) and octadecylamine (ODA) (purity $\geq 99\%$) were also studied. Combining solvent processing with surfactants (OCA and ODA) has been previously reported to result in improved dispersion confirmed by photoluminescence [13]. In this study 0.013 and 0.027 g, respectively, were added to 0.1 g of CNT in 10 mL of solvent equivalent to a 0.1 M solution.

Nitric acid functionalization which imparts carboxyl functionality to the CNTs was also evaluated. One gram of nanotubes were placed in 100 mL of 65% nitric acid and sonicated for 2 h in a sonic bath. The solution was then filtered using a PTFE filter (pore size 0.2 μm) and the CNT collected and dried in a vacuum oven for 48 h at 40°C and 800 millibars pressure [29].

Another treatment investigated was ethanol treatment. This involved mixing 0.1 g of nanotubes in 5 mL of ethanol, dispersing them using a sonic

tip Branson sonifier 250, power level 3 for 3 min constant sonication and then evaporating off the ethanol in a fume cupboard. Although there is a tendency for the CNT to re-agglomerate upon drying, it has reported that there is significant improvement in dispersion from using such treatment [30].

In order to quantify CNT solvent stability, 0.1 g of each CNT type (as-received, nitric functionalized, ethanol treated, OCA and ODA surfactants) were placed in 10 mL of each of the three solvents (THF, NMP, and DMF) resulting in 15 samples. The suspensions were sonicated using a Branson Sonifer 250 for 3 min at setting 3 to ensure the nanotubes were dispersed before a 6 day UV-Vis sedimentation study was undertaken.

CNT/Polysulfone Sample Preparation

Composites were produced at CNT loadings of 0, 1, 3, and 5 wt%. One gram of polysulfone was added to the CNT with 10 mL of solvent and sealed in an airtight container for 48 h to allow the polymer to completely dissolve. The samples were then sonicated continually for 3 min at level three intensity using a Branson Sonifer 250 (THF samples were sonicated under an argon atmosphere). The solutions were then poured into polished aluminum moulds (80 mm × 80 mm) and placed in a fume cupboard at room temperature for THF, and in a temperature controlled oil bath at 35°C for DMF and NMP for 48 h. All samples were further dried in a vacuum oven at 40°C and at 800 millibars pressure for an additional 48 h to remove residual solvent.

Optical and TEM Microscopy

Optical microscope images of the solvent cast samples were obtained at 100× magnification using a Nikon Ellipse 80i microscope fitted with a Nikon E5400 camera and a Nikon MXA 5400 adapter. CNT samples for TEM analysis were prepared by drying CNT dispersions onto a holey carbon coated copper grid. The CNT/Polysulfone samples were prepared for TEM by embedding in epoxy before sections were cut using an ultramicrotome fitted with a diamond knife. The images were taken using at 200 kV using a Jeol 2010.

Tensile Testing

Tensile testing was carried out in accordance with ISO 527 using an Instron 3344 testing machine fitted with a calibrated 2 kN load cell. Samples were cut using a press and a sample cutter, which was manufactured in

compliance with ISO 527 type 5A. Mechanical performance was characterized via Young's modulus.

Electrical Testing

Two metal (titanium) contacts 5 mm apart and 2 mm in diameter were spluttered onto the samples using a suitable mask. The electrical conductivity measurements were measured using a Semilab deep level spectrometer between 20 V and -20 V.

Thermal Analysis

Thermogravimetric analysis (TGA) was conducted between 30°C and 900°C at a ramp rate of 2.5°C/min in air. DSC analysis was conducted on a TA instruments Q100 between 30°C and 400°C at 10°C/min in air. The sample sizes used were approximately 10 mg. The glass transition temperature (T_g) in this study is defined as the inflexion point of the appropriate transition on the DSC trace.

X-ray Photoelectron Spectroscopy

Wide Energy Survey Scans (WESS) were taken over the range of 0–1300 eV binding energy range at a pass energy of 160 eV using a Kratos Axis Ultra DLD spectrometer. High resolution spectra were recorded for C1s and O1s at a pass energy of 20 eV. Any sample charging effects on the measured binding energy positions (eV) were corrected by setting the lowest binding energy component of C1s spectral envelope to 285.0 eV. To allow quantitative analysis, the photoelectron spectra was further processed by subtracting a linear background and using the peak area for the most intense spectral line of each of the determined elemental species to obtain the relative percentage atomic concentrations.

UV-Vis

A sedimentation study was carried out using a Perkin Elmer Labda 11 spectrometer in the range of 800–300 nm with scan intervals of 0.5 nm, each day for 6 days using a 3 mL quartz glass cuvette.

RESULTS AND DISCUSSION

The influence of acid treatment on CNT surface chemistry was investigated using X-ray Photoelectron Spectroscopy (XPS). There was

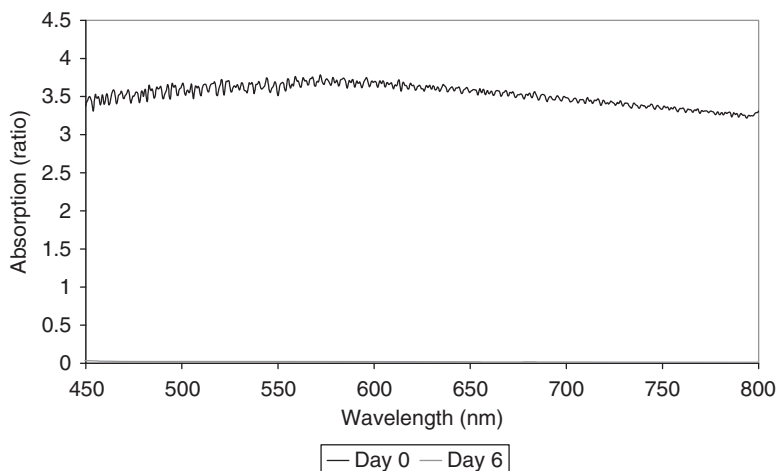


Figure 1. UV-Vis absorption at day 0 and day 6 for NMP.

a significant increase in the amount of oxygen present from 2.58% to 8.27% upon nitric acid functionalization. This signifies that the acid has attacked the tube ends and defect sites and some of the carbon atoms have been replaced with more reactive oxygen. Analysis of the results found that the predominant bonding present was $-C-O$. It has been previously reported that a combination of nitric and sulphuric acids increased surface bond oxygen from 1.1% to 5.2% [29].

The UV-Vis results illustrated in Figures 1–3 show major differences in dispersion behavior between the solvents investigated. Dispersion stability was characterized by the difference in absorbance peak height between day 0 and day 6. Of the three solvents, NMP and DMF displayed dramatically enhanced stability compared to THF, which resulted in a CNT suspension which settled out after several hours. Each of the treatments investigated namely ethanol treatment, nitric functionalization and OCA or ODA surfactants improved dispersion and stability compared to as-received CNT. The dispersion stability of the various CNT treatments in decreasing order characterized by variation of the UV-Vis peak height after 6 days was found to be:

OCA surfactant > ODA surfactant > Nitric Functionalized > Ethanol treated
> As-received

This order was the same for the three solvents tested, but it is worth noting that in the case of the OCA surfactant that the differences between it and the ODA surfactant were minimal. Generally nitric acid functionalized

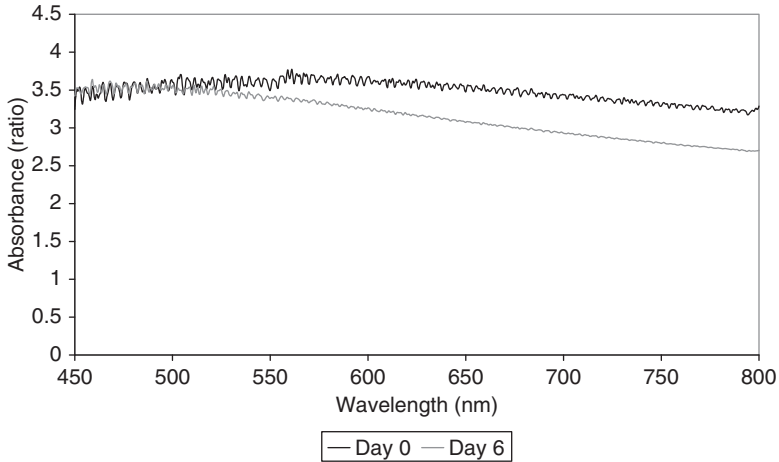


Figure 2. UV-Vis absorption at day 0 and day 6 for THF.

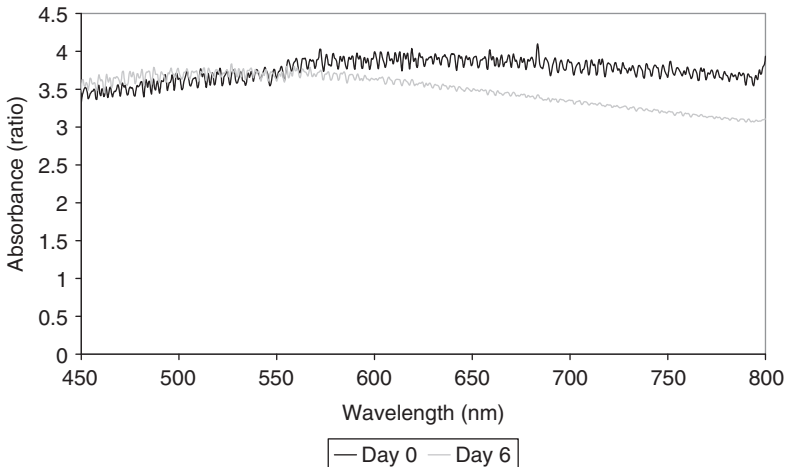


Figure 3. UV-Vis absorption at day 0 and day 6 for DMF.

CNT did not form a stable suspension in solvent, but it was found that in NMP the absorbance was comparable to the two surfactants in terms of stability. The ethanol treated CNT did show a degree of enhanced dispersion in all the solvents compared to the as-received CNT. The as-received CNT exist in large clumps (in the range of $100\mu\text{m}$) and due to their unreactive nature and creating a stable solvent dispersion is problematic. The ethanol treatment assists in breaking the clumps apart. The nitric functionalized

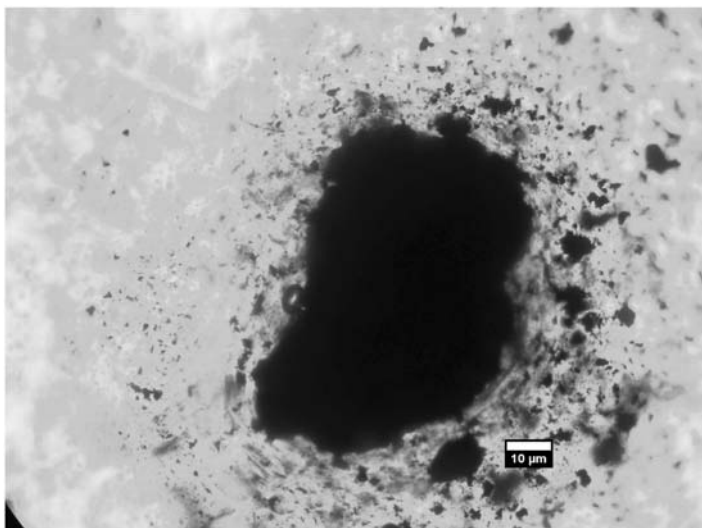


Figure 4. Optical image showing as-received CNT dispersed in THF (3% concentration).

CNT have carboxyl groups which have been reported in literature to concentrate on the ends of the CNT and at defect sites making them more reactive and thus better able to disperse. It has been previously reported that OCA and ODA attach to CNT via the amine group coating the CNT with the free alkane chain enhancing solvent stability [13]. The two surfactants were very close in their ability to enhance the CNT dispersion.

Based on the UV-Vis stability data, 4 CNT/Polysulfone composite sample types were produced: two with THF (as-received and nitric functionalized) and two with NMP (as-received and OCA surfactant). Figures 4–7 show the optical images of the 4 samples produced at 3 wt% CNT concentration at 100 \times . The relative degree of CNT dispersion evident in the composites is in general agreement with the CNT/solubility measured by UV-Vis. The level of dispersion achieved in descending order was:

OCA surfactant NMP > As-received NMP > Nitric Functionalized THF
> As-received THF

The as-received samples in THF showed very poor dispersion and distribution with the CNT present as large agglomerates. The 50–100 μm sized agglomerates in Figure 4 are clearly visible with the naked eye.

The nitric functionalized CNT in THF were much better dispersed than the as-received with the CNT spread throughout the sample as can be seen

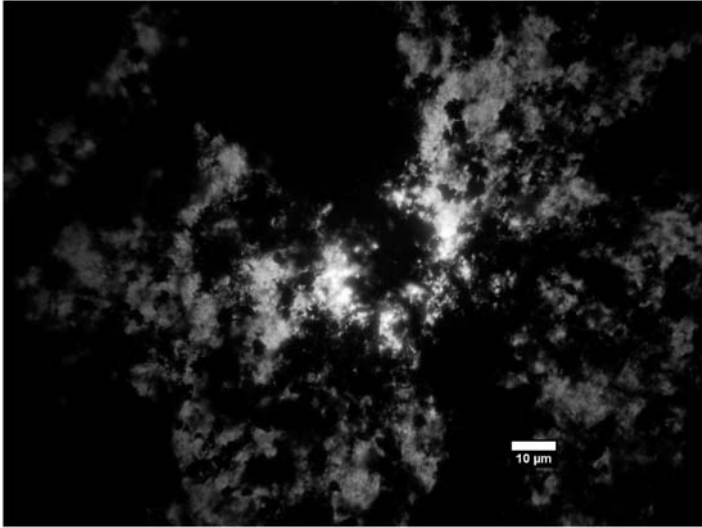


Figure 5. Optical image showing nitric functionalized CNT dispersed in THF (3% concentration).

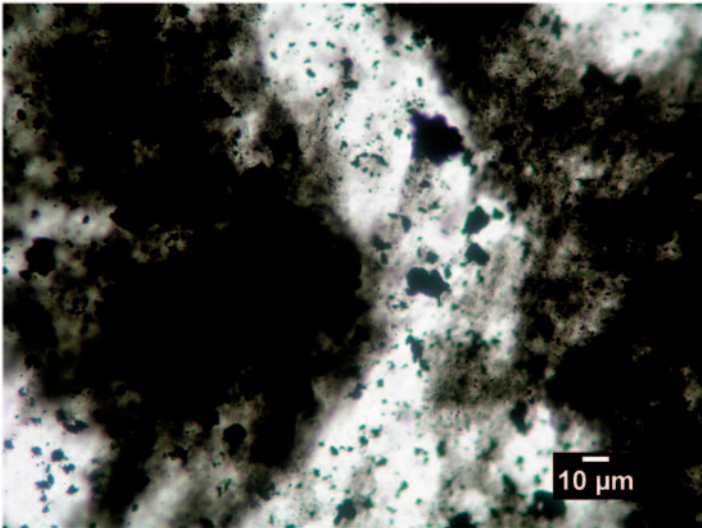


Figure 6. Optical image showing as-received CNT in NMP (3% concentration).

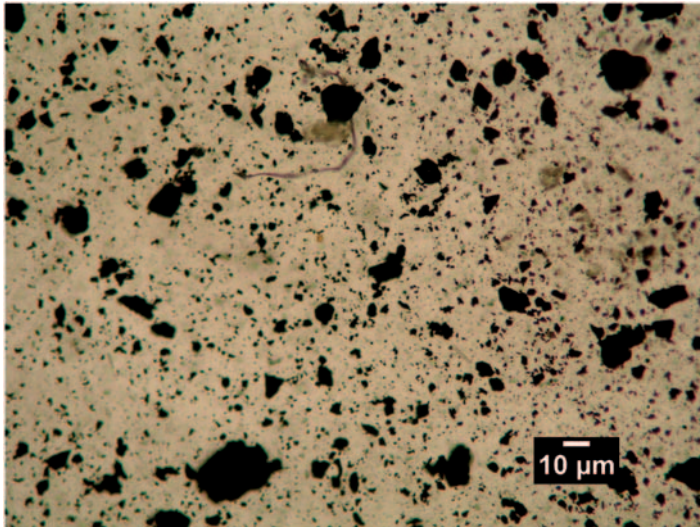


Figure 7. Optical image showing as-received CNT in NMP with an OCA surfactant (3% concentration).

in Figure 5. The dark patches show areas of fine macro level dispersion. A ‘leopard print’ pattern was visible and attributed to water drying effects as THF is extremely hygroscopic. The as-received CNT dispersed in NMP also suffered from relatively poor dispersion with agglomerates in the 10 μm range (Figure 6). However, compared to the samples made using THF, they were more uniform and the samples tended to be a grey color although there were black areas in the sample which although not agglomerates, were areas of high CNT concentration. The best dispersion was achieved with the sample made using CNT dispersed in NMP with the OCA surfactant. Figure 7 shows a typical image taken of the composite and it is clear that it is more uniform and although agglomerates were visible, they tended to be in the 5 μm range or smaller. In addition, the sample was a uniform color and there were no areas of high CNT concentration visible.

TEM images of 3% nitric functionalized composites in THF are shown in Figures 8 and 9. The majority of micrographs of THF processed samples which covered an area of approximately $1 \times 1.5 \mu\text{m}^2$ areas contained no visible CNT. It is presumed that the majority of CNT are present in large agglomerates. Figures 8 and 9 illustrate instances where CNT do exist. Figure 8 shows that some individual tubes do exist within the composite and Figure 9 shows a typical large agglomerate where the majority of CNT are thought to exist.



Figure 8. TEM image of the nitric functionalized CNT dispersed in THF (individual CNTs observed).

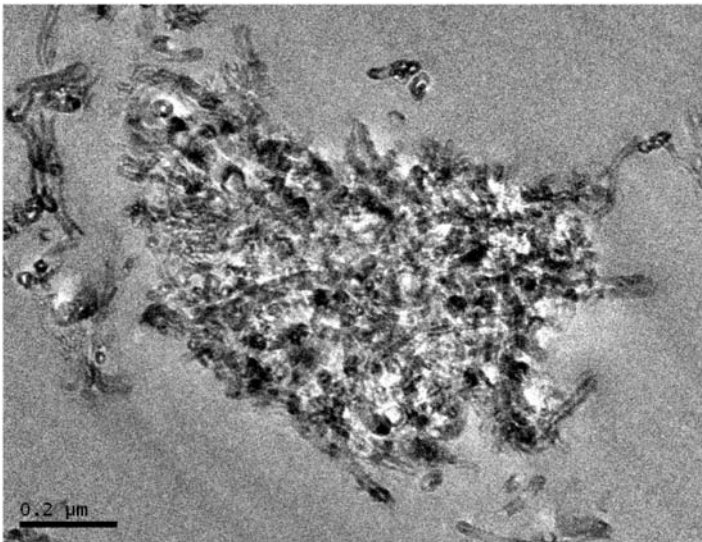


Figure 9. TEM image of the nitric functionalized CNT dispersed in THF (large clumps).

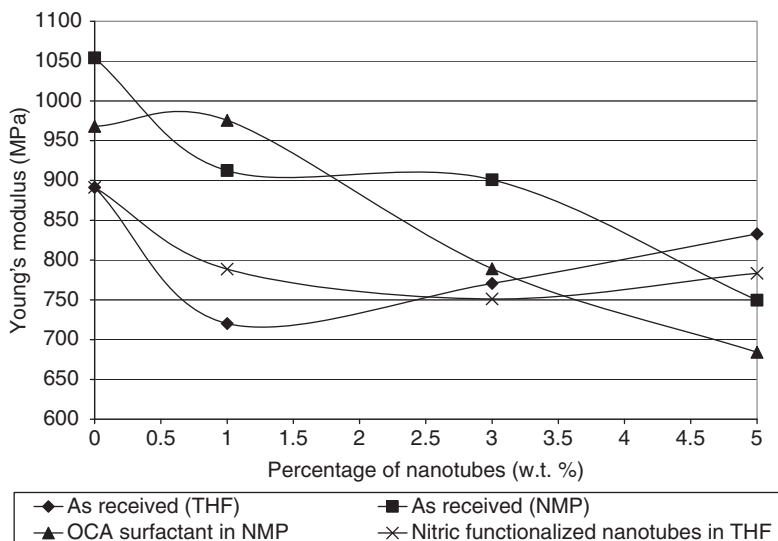


Figure 10. Tensile testing: Young's modulus of the composites.

Tensile testing (Figure 10) showed reduced mechanical performance of the solvent processed sample containing no CNT compared to that expected of polysulfone (2.48 GPa) which is attributed to residual solvent. In general agreement with the UV-Vis and microscope data, the NMP prepared composites displayed improved stiffness compared to those prepared using THF. Neither the addition of surfactant or nitric functionalization had a significant effect on Young's modulus compared to untreated CNT. It is noted that at high CNT concentrations THF prepared composites displayed improved stiffness. It would also appear that the addition of the surfactant had a detrimental effect on the mechanical properties as evidenced by the drop in stiffness in the sample made with NMP but no CNT.

The electrical testing results depicted in Table 1 show that the percolation point is several orders of magnitude higher than that predicted for a CNT composite with perfect dispersion. The theoretical value for straight randomly aligned perfectly dispersed CNT with a diameter and length of 15 nm and 10 μm is a volume fraction of 2.15×10^{-5} equivalent to 0.0023 wt% [31]. A percolation point of 3% was recorded for the as-received CNT prepared using NMP. This compares to a percolation threshold of 5% for the two sample types prepared using THF. This further illustrates the enhanced dispersion resulting from the use of NMP. It is interesting to note the insulating behavior observed in the samples containing OCA surfactant.

Table 1. Resistivity conductivity of the samples (Ω/m).

Sample type	Concentration			
	0%	1%	3%	5%
As received (THF)	Insulating	Insulating	Insulating	21.74
Nitric functionalized (THF)	Insulating	Insulating	Insulating	40.36
As received (NMP)	Insulating	Insulating	Nonlinear conducting	7833.33
OCA surfactant (NMP)	Insulating	Insulating	Insulating	Insulating

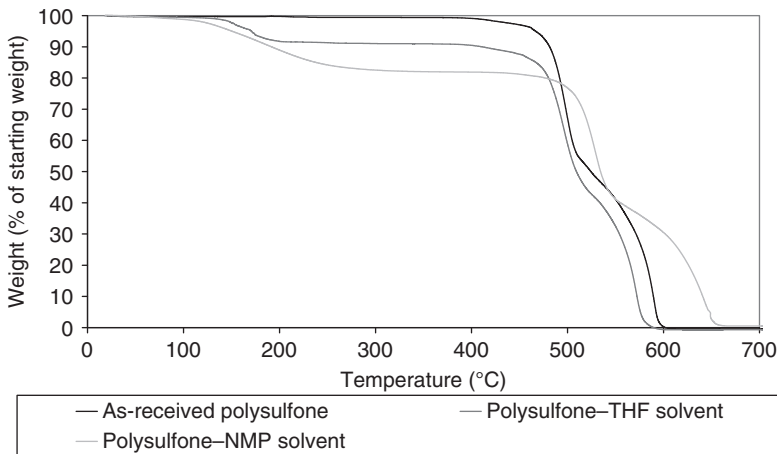


Figure 11. TGA for polysulfone.

The improved dispersion observed optically did not translate into improved electrical conductivity which is attributed to the surfactant coating the CNT, which would have an insulating effect.

Figure 11 shows the TGA curves for the pure polysulfone powder, and the polysulfone processed using each of the two solvents with no CNT added. TGA confirms high levels of residual solvent of between 12–20% evidenced by the weight loss occurring at $\sim 200^\circ\text{C}$ for the NMP samples. This shows the drying of the samples was inadequate. Comparison between the 0% (no nanotubes present) and the 3% CNT concentration sample showed that there was no significant difference in the amount of solvent in the sample regardless of CNT loading. However, with the THF samples, the weight loss was between 7% and 8% occurring at approximately 150°C .

The DSC data given in Table 2 shows that the glass transition temperature (T_g) of the composites is much lower than the polysulfone

Table 2. DSC results showing glass transition (T_g) temperatures.

Solvent	Composite type	Glass Transition ($^{\circ}$ C)
None	Polysulfone (as received)	186
THF	0% CNT	94
NMP	0% CNT	70
NMP	0% CNT with OCA surfactant	64

prior to solvent processing. This is indicative of the plasticizing effect of residual solvent. It is not possible to determine what effect the addition of the CNT had on the glass transition temperature since the effect of residual solvent dominates.

Several researchers have turned to using solubility parameters (such as the Hildebrand solubility parameter) in order to predict which treatments can be applied to the CNT in order to make them soluble in solvents. Although these solubility parameters can be used to highlight suitable functionalization approaches. Ideally, a functionalization approach could be identified which would allow the CNT to be fully solvated with both the solvent to obtain a good dispersion and the polymer polysulfone has a solubility parameter of approximately $22 \text{ MPa}^{-0.5}$ [32,33], NMP has a solubility parameter of $23 \text{ MPa}^{-0.5}$, DMF $24.8 \text{ MPa}^{-0.5}$, and THF $18.6 \text{ MPa}^{-0.5}$ [34]. OCA has a calculated value of $19 \text{ MPa}^{-0.5}$, which explains why it is an effective surfactant. Further work will focus on identifying and attaching chemical groups to the CNT which have a solubility parameter matching polysulfone such as PMMA with a solubility parameter of $22.6 \text{ MPa}^{-0.5}$ [35]. Given the potential of solubility parameters, further work will focus on the predictions made by them.

CONCLUSIONS

The influence of a range of CNT treatments namely OCA and ODA surfactants, nitric acid and ethanol treatment on stability in NMP, THF, and DMF were investigated via UV-Vis. Based on this testing, it was found that DMF and NMP resulted in a more stable dispersion as compared to THF. All of the treatments investigated resulted in improved stability relative to the as-received CNT, with the surfactants having the greatest effect. Four CNT/polysulfone sample types were produced and optical microscopy imaging found similar relative effects of CNT treatment and solvent choice on CNT dispersion. This study has shown CNT solvent stability has an influence on the dispersion achieved in the final composite. It was noted that a relatively poor dispersion was observed in all samples with micron-sized agglomerates present.

TGA analysis revealed significant levels of residual solvent in the composite samples. Differences in the levels of solvent between samples processed using NMP and THF makes direct comparisons difficult. Although the drying times were adequate for the THF samples, further drying is required for the NMP due to its higher boiling point. The temperature and duration a polymer is subjected to heat does lead to degradation and thus for this study the composites were produced in exactly the same way in order to combat this. The solvent levels had a large influence on the mechanical performance and their plasticizing effect reduced the T_g considerably. Total solvent removal is not practical and previous studies have reported residual solvent after a period of 2 years [36]. Despite the critical nature of solvent removal, it is interesting to note that in a surprising number of papers published this aspect is overlooked. As a consequence it can be said that it is difficult if not impossible to make comparisons between composites made from different polymers or even different solvents using the solution method as so much depends on solvent removal.

ACKNOWLEDGEMENTS

The project was funded by the Department of Employment and Learning (DEL) in Northern Ireland. The use of the TEM was possible thanks to the EPSRC Access Program EP/F01919X/1 and the Department of Materials, University of Oxford. The polymer used was donated by Solvay advanced Polymers.

REFERENCES

1. Iijima, S. (1991). Helical Microtubules of Graphitic Carbon, *Nature*, **354**: 56–58.
2. Wong, E.W., Sheehan, P.E. and Lieber, C.M. (1997). Nanobeam Mechanics: Elasticity, Strength, and Toughness of Nanorods and Nanotubes, *Science*, **277**: 1971–1975.
3. Yu, M., Lourie, O., Dyer, M.J., Moloni, K., Kelly, T.F. and Ruoff, R.S. (2000). Strength and Breaking Mechanism of Multiwalled Carbon Nanotubes under Tensile Load, *Science*, **287**: 637–640.
4. Wei, B.Q., Vajtai, R. and Ajayan, P.M. (2001). Reliability and Current Carrying Capacity of Carbon Nanotubes, *Applied Physics Letters*, **79**(8): 1172–1174.
5. Pang, L.S.K., Saxby, J.D. and Chatfield, S.P. (1993). Thermogravimetric Analysis of Carbon Nanotubes and Nanoparticles, *The Journal of Physical Chemistry*, **97**(27): 6941–6942.
6. Shao, Y., Yin, G., Zhang, J. and Gao, Y. (2006). Comparative Investigation of the Resistance to Electrochemical Oxidation of Carbon Black and Carbon Nanotubes in Aqueous Sulphuric Acid Solution, *Electrochimica Acta*, **51**: 5853–5857.
7. Hata, K., Futaba, D.N., Mizuno, K., Namai, T., Yumura, M. and Iijima, S. (2004). Water-assisted Highly Efficient Synthesis of Impurity-free Single-walled Carbon Nanotubes, *Science*, **306**: 1362–1364.

8. Kalaugher, L. (2005). Nanotube Bike Enters Tour de France. Available at: <http://nanotechweb.org/cws/article/tech/22597> (accessed date March 22, 2010).
9. Pötschke, P., Bhattacharyya, A.R., Janke, A. and Goering, H. (2003). Melt Mixing of Polycarbonate/Multi-walled Carbon Nanotubes Composites, *Composites Interfaces*, **10**(4–5): 389–404.
10. Breuer, O. and Sundararaj, U. (2004). Big Returns from Small Fibers: A Review of Polymer/Carbon Nanotube Composites, *Polymer Composites*, **25**(6): 630–645.
11. Lambin, P.H., Loiseau, A., Culot, C. and Biró, L.P. (2002). Structure of Carbon Nanotubes Probed by Local and Global Probes, *Carbon*, **40**: 16335–1648.
12. Giodani, S., Bergin, S.D., Nicolosi, V., Ledebkin, S., Kappes, M.M., Blau, W.J. and Coleman, J.N. (2006). Debundling of Single-walled Nanotubes by Dilution: Observation of Large Populations of Individual Nanotubes in Amide Solvent Dispersion, *Journal Physical Chemistry B*, **110**: 15708–15718.
13. Maeda, Y., Kimura, S., Hirashima, Y., Kanda, M., Lian, Y., Wakahara, T., Akasaka, T., Hasegawa, T., Tokumoto, H., Shimizu, T., Kataura, H., Miyauchi, Y., Maruyama, S., Kobayashi, K. and Nagase, S. (2004). Dispersion of Single-walled Carbon Nanotube Bundles in Nonaqueous Solution, *Journal of Physical Chemical B*, **108**: 18395–18397.
14. Chen, G., Kim, H., Park, B.H. and Yoon, J. (2006). Multi-walled Carbon Nanotubes Reinforced Nylon 6 Composites, *Polymer*, **47**: 4760–4767.
15. Brydson, J.A. (1989). *Plastic Materials*, **5th edn**, pp. 173–175, Butterworth Heinemann, Oxford.
16. Coleman, J.N., Khan, U. and Gun'ko, Y.K. (2006). Mechanical Reinforcement of Polymers using Carbon Nanotubes, *Advanced Materials*, **18**: 689–706.
17. Calvert, P. (1999). Nanotube Composites: A Recipe for Strength, *Nature*, **399**: 210–211.
18. Curran, S.A., Ajayan, P.M., Blau, W.J., Carroll, D.L., Coleman, H.N., Dalton, A.B., Davey, A.P., Drury, A., McCarthy, B., Maier, S. and Strevens, A. (1998). A Composite From Poly(m-phenylenevinylene-co-2,5-dioxy-p-phenylenevinylene) and Carbon Nanotubes: a Novel Material for Molecular Optoelectronics, *Advanced Materials*, **10**(14): 1091–1093.
19. Schadler, L.S., Giannaris, S.C. and Ajayan, P.M. (1998). Load Transfer in Carbon Nanotube Epoxy Composites, *Applied Physics Letters*, **73**(26): 3842–3844.
20. Cadek, M., Coleman, J.N., Barron, V., Hedicke, K. and Blau, W.J. (2002). Morphological and Mechanical Properties of Carbon-Nanotube-Reinforced Semicrystalline and Amorphous Polymer Composites, *Applied Physics Letters*, **81**(27): 5123–5125.
21. Cadek, M., Coleman, J.N., Ryan, K.P., Nicolosi, V., Bister, G., Fonseca, A., Nagy, J.B., Szostak, K., Béguin, F. and Blau, W.J. (2004). Reinforcement of Polymers with Carbon Nanotubes: the Role of Nanotube Surface Area, *Nano Letters*, **4**(2): 353–356.
22. Coleman, J.N., Cadek, M., Blake, R., Nicolosi, V., Ryan, K.P., Belton, C., Fonseca, A., Nagy, J.B., Gun'ko, Y.K. and Blau, W.J. (2004). High-performance Nanotube-reinforced Plastics: Understanding the Mechanism of Strength Increase, *Advanced Functional Materials*, **14**(8): 791–798.
23. Dufresne, A., Paillet, M., Putaux, J., Canet, R., Carmona, F., Delhaes, P. and Cui, S. (2002). Processing and Characterization of Carbon Nanotube/Poly(styrene-co-butyl acrylate) Nanocomposites, *Journal of Materials Science*, **37**: 3915–3923.
24. Qian, D., Dickey, E.C., Andrews, R. and Rantell, T. (2000). Load Transfer and Deformation Mechanisms in Carbon Nanotube-Polystyrene Composites, *Applied Physics Letters*, **76**(10): 2868–2870.
25. Safadi, B., Andrews, R. and Gruke, E.A. (2001). Multiwalled Carbon Nanotubes Polymer Composites: Synthesis and Characterization of Thin Films, *Journal of Applied Polymer Science*, **84**: 2660–2669.

26. Harris, J.E. and Rubin, I.I. (ed.) (1990). *Handbook of Plastic Materials and Technology*, Wiley-Interscience Publication, pp. 487–499, John Wiley and Sons Incorporated, New York.
27. Sánchez, S., Pumera, M. and Fàbregas, E. (2007). Carbon Nanotube/Polysulfone Screen-printed Electrochemical Immunosensor, *Biosensors and Bioelectronics*, **23**: 332–340.
28. Kim, S., Chen, L., Johnson, J.K. and Marand, E. (2007). Polysulfone and Functionalized Carbon Nanotube Mixed Matrix Membranes for Gas Separation: Theory and Experiment, *Journal of Membrane Science*, **294**: 147–158.
29. S.-T. Lin, K.-L. Wei, T.-M. Lee, K.-C. Chiou and J.-J. Lin (2006). Functionalizing Multi-walled Carbon Nanotubes with Poly(oxyalkylene)-Amidoamines, *Nanotechnology*, **17**: 3197–3203.
30. S. Bal (2007). Influence of Dispersion States of Carbon Nanotubes on Mechanical and Electrical Properties of Epoxy Nanocomposites, *Journal of Scientific and Industrial Research*, **66**(9): 752–756.
31. Li, J., Ma, P.C., Chow, W.S., To, C.K., Tang, B.Z. and Kim, J. (2007). Correlations between Percolation Threshold, Dispersion State, and Aspect Ratio of Carbon Nanotubes, *Advanced Functional Materials*, **17**: 3207–3215.
32. Lencki, R.W. and Williams, S. (1995). Effect of Nonaqueous Solvents on the Flux Behaviour of Ultrafiltration Membranes, *Journal of Membrane Science*, **101**: 43–51.
33. Rajagopalan, G., Immordino, K.M., Gillespie, J.W. Jr. and McKnight, W.H. (2000). Diffusion and Reaction of Epoxy and Amine in Polysulfone Studied Using Fourier Transform Infrared Spectroscopy: Experimental Results, *Polymer*, **41**: 2591–2602.
34. Barton, A.F.M. (1975). Solubility Parameters, *Chemical Reviews*, **75**(6): 731–753.
35. Lindvig, T., Michelsen, M.L. and Kontogeorgis, G.M. (2007). A Flory-Huggins Model Based on the Hansen Solubility Parameters, *Fluid Phase Equilibria*, **203**: 247–260.
36. Freier, T., Kunze, C. and Schmitz, K.P. (2001). Solvent Removal from Solution-cast Films of Biodegradable Polymers, *Journal of Materials Science Letters*, **20**: 1929–1931.